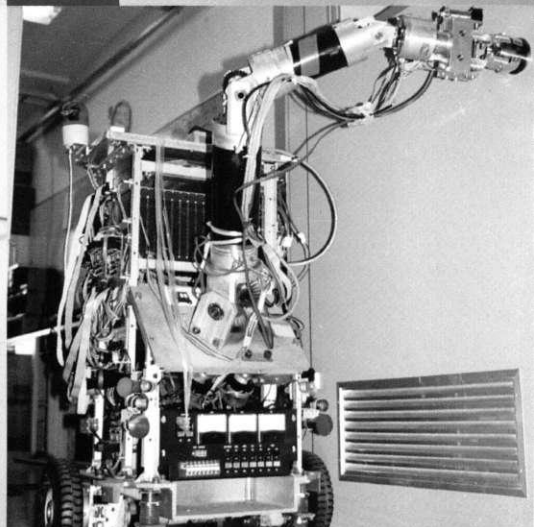
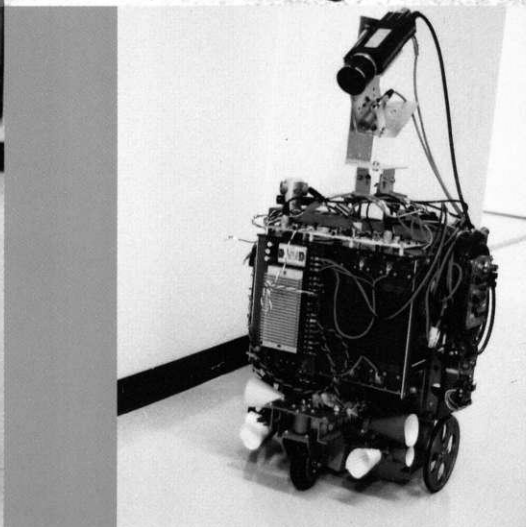
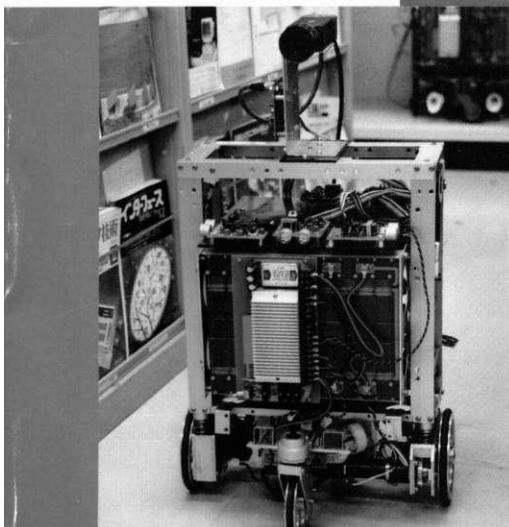
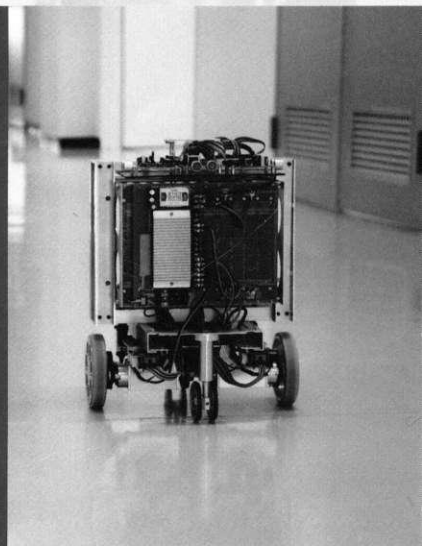
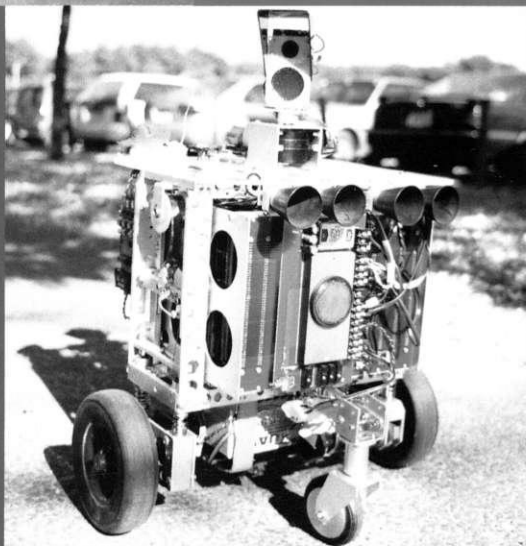
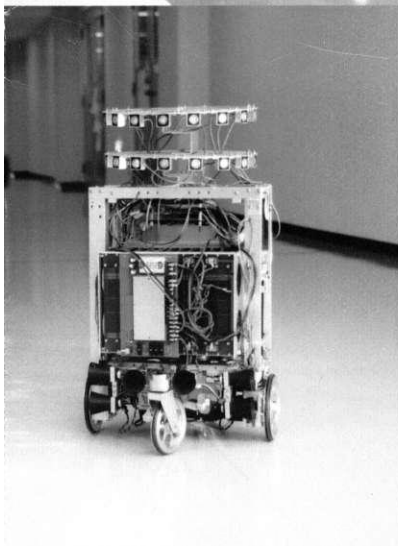
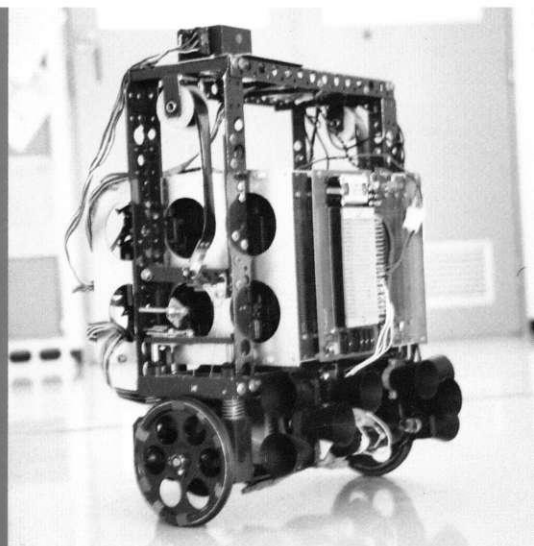
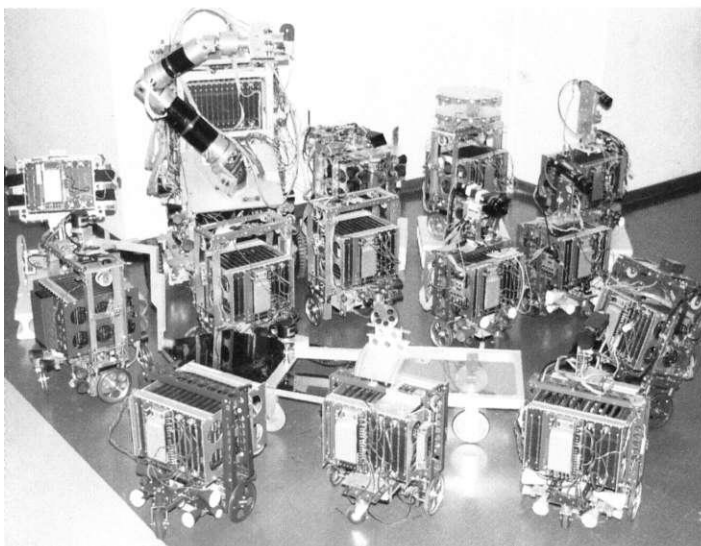


# Journal of Robotics and Mechatronics

Vol.8 No.6 Dec. 1996

■ Special Issue on Integration of Intelligence for Robotics in VLSI Chips



Paper:

# Study of the Stability and Motion Control of a Unicycle (5th Report: Experimental Results by Fuzzy Gain Schedule PD Controllers)

Zaiquan Sheng\*, Kazuo Yamafuji\* and Sergei V. Ulyanov\*

\* Department of Mechanical and Control Engineering, University of Electro-communications  
1-5-1 Chofugaoka, Chofu Tokyo, 182 Japan

[Received August 19, 1996; accepted October 20, 1996]

In this paper, the use of three gyrosensors for detection of a unicycle robot's posture in three dimensions, and experiments on the unicycle robot's postural stability control are conducted with fuzzy gain schedule PD control. Experimental results show that both the robot's longitudinal and lateral posture can be stabilized successfully. Comparing the experimental results with one PD and one D controller, those by two fuzzy gain schedule PD controllers are much better. Real-time experimental results indicate that the fuzzy gain schedule PD control proposed here is quite effective in robot postural stability control. Experimental results also show that proposed fuzzy gain schedule PD control provides a reasonable approach to handling nonlinear problems that exist in the system.

**Keywords:** Unicycle, Postural stability, Fuzzy gain schedule PD controller, 3D posture, Gyrosensors, Longitudinal and lateral stability

## 1. Introduction

It is well-known that the unicycle system is inherently unstable, and both longitudinal and lateral stability control are simultaneously needed to maintain the unicycle's postural stability. It is an unstable problem in three dimensions. However, a human rider can obtain postural stability on a unicycle, keep the wheel's movement speed as a constant value, and change unicycle posture in a yaw direction as desired by using bodily flexibility, good sensory systems, skill, and intelligence. In the investigation of this mechanisms and emulation of the system by a robot, we construct a model of human motion dynamics, and test new control methods for stability control and system analysis.

From the observation of a human riding a unicycle, we know that the rider's posture on the unicycle is always changing. It is necessary for us to define postural stability in this system. Usually, if a system is stabilized, some variables in that system will be controlled as constant. However, because the unicycle system is an inherently unstable system, and postural stability is achieved by centrifugal force created by the rider's dynamic action. Pitch, roll, and yaw angles are always changeable, so it is impossible for the rider to maintain these three variables constant. From the observation of a human riding a unicycle, we know that the change of yaw angle relates to stability control of the

roll angle, and if the roll angle changes, the yaw angle will also change. The change of pitch and roll angle is often within some range. The biggest possible range is 90 degrees. However from the observation of a human riding a unicycle, postural stability is often broken if either pitch or roll angle becomes bigger than about 16 degrees. If there is not enough centrifugal force created by control in this system, postural stability fails about 1 second. If there is no control, postural stability fails quickly. This means that, if postural stability is maintained longer than 1 second, control action is acting on the system.

Basing on the characteristics of posture change in unicycle system, we can define unicycle postural stability as follows:

1. Neither pitch angle nor roll angle increases. Usually both pitch and roll angle can be changed, but the change is within some range (the biggest range is 90 degrees. Because of the power limit of motor in an unicycle robot, the range will be much less than 90 degrees).
2. Posture should be maintained at least longer than 1 second.

In our first report<sup>1)</sup>, a new model is proposed (Fig.1). In this model, a closed link mechanism is used for control of pitch, and a turntable for control of roll. As reported<sup>1)</sup>,

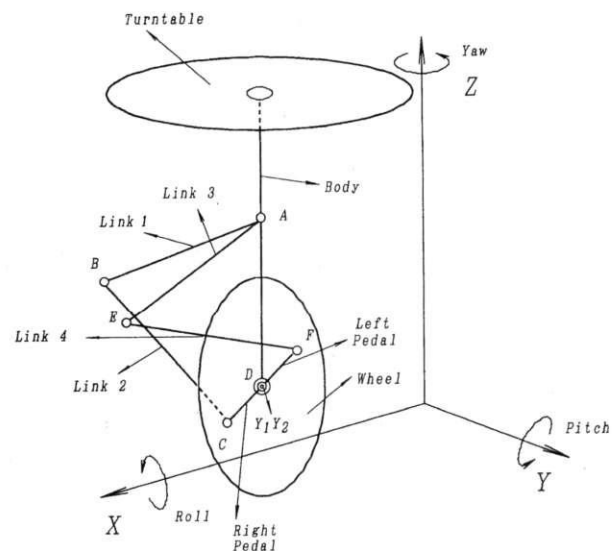


Fig. 1. Robot's model emulating human riding unicycle.

patterns 1 and 2 drive closed link mechanisms. In pattern 1, as shown in Fig.1, two motors are used at joining A1 and A2 to drive link 1 and link 3. In this pattern, the wheel is driven by two motors and stability in pitch is also obtained by these two motors. From the point of control, it is not suitable to use a motor for driving the wheel and getting stability in pitch at the same time. In pattern 2, three motors are used. One motor (motor 1) is for wheel drive, and other two motors (motor 3 and motor 4) are used to drive links 2 and 4. These two motors for links 2 and 4 are fixed at joints C and F. The robot's stability in pitch is expected to be obtained by the control on links 2 and 4. As analyzed in our first report,<sup>1)</sup> since the structure with two closed link mechanisms has only two degrees of freedom, two actuators are enough for its control. That means one of three motors (motors 1, 3, and 4) can be omitted in pattern 2. We can omit motor 1 and use motors 3 and 4, or we can omit motor 3 or 4 and use motors 1, 4, or 3. If we omit motor 1 and use motors 3 and 4 for wheel drive and pitch stability control, from the point of control, it will become complicated for the determination of torque in motors 3 and 4. If we omit motor 3 and use motors 1 and 4, the torque to motors 3 and 1 can be decided easily. The torque to motor 3 is for pitch stability control, and the torque to motor 1 is for wheel drive. Only for the structure's symmetry and balance, motor 3 is added, in this case, because three actuators are used for control of the structure with two degrees of freedom. The structure becomes a redundant system. We have analyzed when the structure is driven by two motors (motors 1 and 4) or three motors (motors 1, 3, and 4) in pattern 2, we found analytical results are similar. The only difference is the requirement of the motor's driving torque. Considering the structure's symmetry and balance, we recognized that the pattern with three motors will be more practical than the pattern with two motors, and it is easier for us to design an unicycle robot using the pattern with three motors. For the above reasons, we propose to use two motors to drive links 2 and 4. The torque for these two motors are taken as the same for the consideration of structure redundancy and for simplicity, and use one motor to drive the wheel directly. From the result in the first report,<sup>1)</sup> pattern 2 is more practical than pattern 1, so our unicycle robot is designed and developed based on pattern 2 in our second report.<sup>2)</sup>

Experimental results are given in our second report<sup>2)</sup> and another paper.<sup>14)</sup> Based on the preparatory experiment, the model was improved by making the turntable asymmetric instead of symmetric. In our third report,<sup>3)</sup> the characteristics of the developed unicycle robot are analyzed, and nonlinearity of the unicycle robot is demonstrated.

In handling nonlinear problems, many different approaches are taken by different researchers. Control results achieved through different fuzzy control methods proposed by researchers<sup>4-12)</sup> show that fuzzy control methodology is a possible approach for nonlinear problems, but most work conducted by researchers is on theory, and fuzzy tuning speed is not usually fast. Real-time control needs simple and active fuzzy controllers. For handling the nonlinear unicycle robot problem, a new fuzzy gain schedule PD controller is developed in our fourth report,<sup>13)</sup> and simulation results by different control patterns show that our proposed method is effective in handling the nonlinear unicycle robot problem.

In this paper, the best control pattern (two fuzzy gain

schedule PD controllers) is applied to unicycle robot postural stability control in real-time experiments. Experimental results show that the proposed method can make the robustness of the robot's postural stability control better. The validity of the proposed method is demonstrated in experiments.

## 2. Unicycle Robot and Detection of Its Posture

The manufactured unicycle robot with an asymmetric rotor is shown in Fig.2. It is composed of a wheel with two cranks, a main body, an overhead rotor, and two closed links on both sides of the wheel. The closed link mechanism is used for longitudinal stability and the asymmetric rotor for lateral robot stability. Four motors are used. The wheel is driven through a ball reduction gear, a couple of spiral bevel gears and a timing belt by a DC servomotor (60w) mounted inside the robot (motor 1 in Fig.2).

The rotor is driven by a harmonic drive motor (34w) installed on the body (motor 2 in Fig.1). The left and right closed link are driven directly by a harmonic drive motor (20.3w) on links 2 and 4 (motors 3 and 4 in Fig.2). Motor 3 is the same as motor 4 for the structure's geometric symmetry and balance of the robot.

The structure of the asymmetric rotor is detailed in our previous papers.<sup>2,3)</sup>

Figure 3 is a block diagram of control system. A 32-bit personal computer is used for the system controller. The wheel, asymmetric rotor, and closed link mechanisms are driven through torque controlled to motors with software-servo control, and all control programs are written in C language.

As shown in Fig.2, there are three rategyrosensors (sensors A, B, and C) mounted on the three principal axes of the robot's body for measuring angular velocities of body inclination in the direction of pitch, roll, and yaw. The resolution of the angular velocity of the rategyrosensor is 0.1 degree/second. An optical rotary encoder (500 pulses/revolution) is installed on each servomotor to detect the rotation angle caused by the rotation of servomotor. As in our previous paper,<sup>2)</sup> the usage of coordinates defined in Fig.4 for the robot enables us to calculate the robot's posture or Euler's angle ( $\alpha, \beta, \gamma$ ) related to the global reference coordinate from measured angular velocity  $\omega_x, \omega_y,$  and  $\omega_z$  by the three gyrosensors in Eqs.(1)-(3),

$$\alpha = \int ((\omega_x \cos \beta - \omega_x \sin \beta) \cos^{-1} \gamma) dt \dots \dots (1)$$

$$\beta = \int (\omega_y - (\omega_z \cos \beta - \omega_x \sin \beta) \tan \gamma) dt \dots (2)$$

$$\gamma = \int (\omega_x \cos^{-1} \beta + (\omega_z \cos \beta - \omega_x \sin \beta) \tan \beta) dt \dots \dots (3)$$

where  $\omega_y$  : angular velocity related to  $px_6$

$\omega_y$ : angular velocity related to  $py_6$   
 $\omega_z$ : angular velocity related to  $pz_6$

Usually, there is drift on the output of this kind of small rategyrosensor due to time and change of temperature. The drift may yield unfavorable influence on calculation of the postural angles in experiments. Thus, rategyrosensors with the least drift are selected from rategyrosensors. Experiments are conducted within about 8 seconds because the drift of the gyrosensor's output within 8 seconds is not large.

### 3. Control Method and Experimental Results

The experiment is carried out on the unicycle robot by using the control methods proposed in the previous paper.<sup>13)</sup> The robot's wheel is made of aluminum, not rubber. To make it easier for control and to make friction between wheel and ground bigger to keep the wheel from slipping, the experiment is conducted on a 3.0m×9.0m synthetic rub-

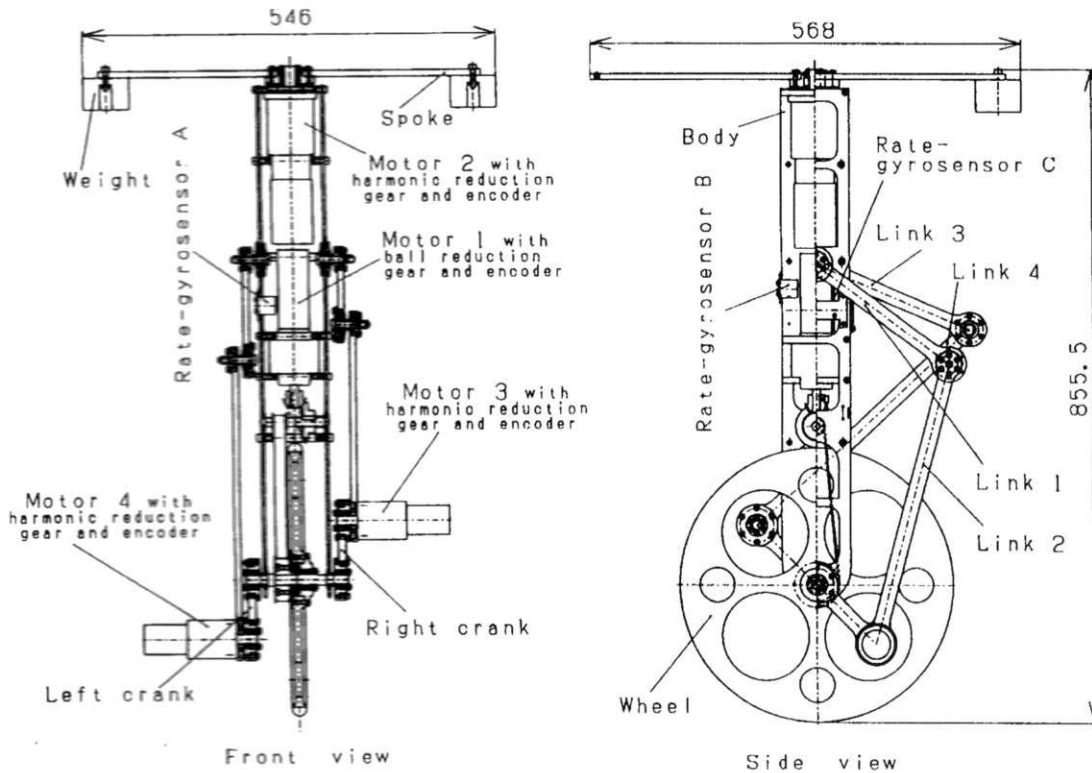


Fig. 2. Manufactured unicycle robot with asymmetric rotor.

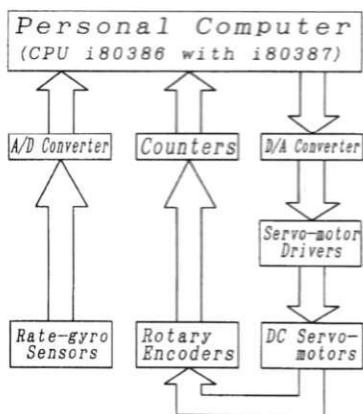


Fig. 3. Block diagram of control system.

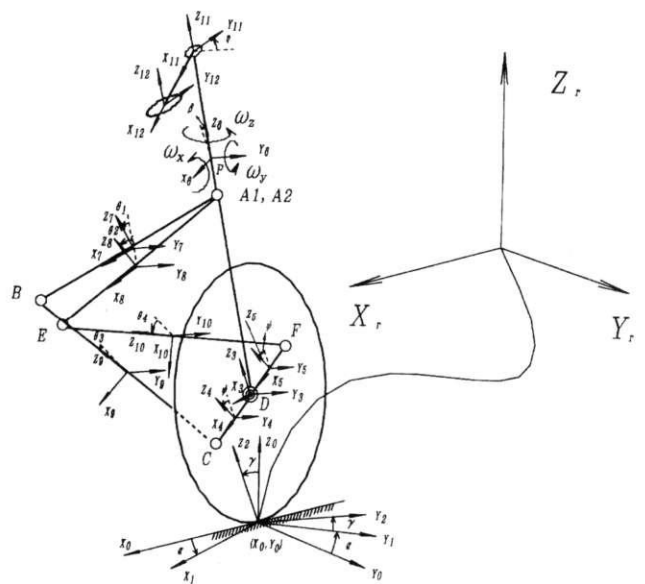


Fig. 4. Coordinate systems defined on the robot.

ber carpet. Control and experimental results are reported below.

As pointed out in our previous study,<sup>1,4)</sup> the robot's postural stability control is not so dependent on wheel movement and the wheel is used for giving the unicycle system a forward speed. Thus, a simple control method in Eq.(4) for helping the wheel overcome friction gives the wheel speed,

$$\tau_\psi = A \dots \dots \dots (4)$$

where  $\tau_\psi$  is wheel torque and  $A$  is a constant value.

As proposed in a previous paper,<sup>13)</sup> fuzzy gain schedule PD control is used for links 2 and 4. The torque applied to link 2 is same as to link 4. Because motors 3 and 4 are fixed on links 2 and 4 symmetrically, the clockwise revolution of motors 3 and 4 are opposite, we must calculate torque for motor 3 as in Eq.(5) and torque for motor 4 as in Eq.(6) to apply the same torque to motors 3 and 4,

$$\tau_{\theta_2} = -kp_1 \times k_1 \times \beta - kd_1 \times k_2 \times \dot{\beta} \dots \dots \dots (5)$$

$$\tau_{\theta_4} = -\tau_{\theta_2} \dots \dots \dots (6)$$

where  $\tau_{\theta_2}$  and  $\tau_{\theta_4}$  are torque for links 2 and 4;  $kp_1$  and  $kd_1$  are constant feedback gains; and  $k_1$  and  $k_2$  are changeable parameters.

Fuzzy gain schedule PD control to the rotor is given in Eq.(7),

$$\tau_\eta = kp_2 \times k_3 \times \gamma + kd_2 \times k_4 \times \dot{\gamma} \dots \dots \dots (7)$$

where  $\tau_\eta$  is torque to the rotor;  $kp_2$  and  $kd_2$  are constant feedback gains; and  $k_3$  and  $k_4$  are changeable parameters.

In Eqs.(5) and (7),  $k_1, k_2, k_3,$  and  $k_4$  are varied between 0.0 and 1.0, and are determined by fuzzy rules and reasoning. The membership functions for  $\beta, \dot{\beta}, \gamma,$  and  $\dot{\gamma}$  are shown in Fig.5. In Fig.5, N represents negative, P positive, ZO zero, S small, M medium, and B big. NM stands for negative medium, PB for positive big, and so on. Fuzzy variables are computed in the form of  $\beta/\beta_m, \dot{\beta}/\dot{\beta}_m, \phi/\phi_m$  or  $\dot{\gamma}/\dot{\gamma}_m$ . In experiments,  $\beta_m, \dot{\beta}_m, \gamma_m,$  and  $\dot{\gamma}_m$  are chosen as 0.2 rad, 0.8rad/s, 0.2 rad, and 0.8 rad/s.

The output membership functions for  $k_1, k_2, k_3,$  and  $k_4$  are displayed in Fig.6. The fuzzy tuning rules for  $k_1, k_2, k_3,$  and  $k_4$  are shown in Tables 1, 2, 3, and 4. In tables, B stands for Big and S for Small.

The truth value of the  $i$ th rule in the consequence part for  $k_1, k_2, k_3,$  and  $k_4$  are obtained by the product of membership functions values in the antecedent of the rule as Eqs.(8), (9), (10), and (11),

$$\mu_{i,k_1} = \mu_\beta(\beta_i) \cdot \mu_{\dot{\beta}}(\dot{\beta}_i) \dots \dots \dots (8)$$

$$\mu_{i,k_2} = \mu_{i,k_1} \dots \dots \dots (9)$$

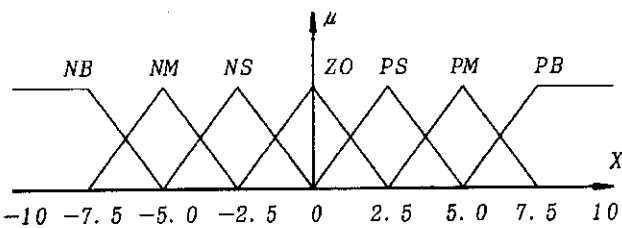


Fig. 5. Membership functions for input variables.

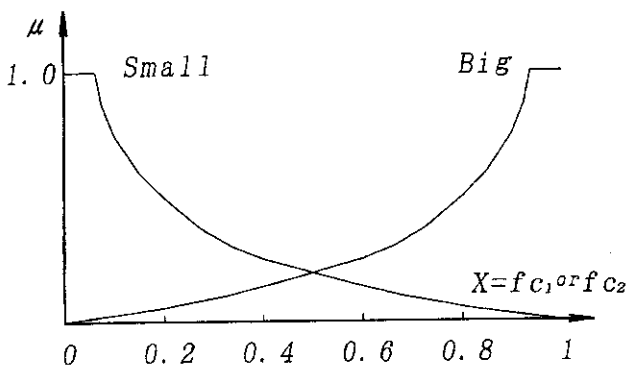


Fig. 6. Membership functions for output variables.

Table 1. Fuzzy tuning rules for  $k_1$ .

$\delta\beta / \delta\dot{\beta}$	NB	NM	NS	ZO	PS	PM	PB
NB	S	B	B	B	B	B	S
NM	S	B	B	B	B	B	S
NS	S	S	B	B	B	S	S
ZO	S	S	S	B	S	S	S
PS	S	S	B	B	B	S	S
PM	S	B	B	B	B	B	S
PB	S	B	B	B	B	B	S

Table 2. Fuzzy tuning rules for  $k_2$ .

$\delta\beta / \delta\dot{\beta}$	NB	NM	NS	ZO	PS	PM	PB
NB	S	S	S	S	S	S	S
NM	B	B	S	S	S	B	B
NS	B	B	B	S	B	B	B
ZO	B	B	B	B	B	B	B
PS	B	B	B	S	B	B	B
PM	B	B	S	S	S	B	B
PB	S	S	S	S	S	S	S

**Table 3.** Fuzzy tuning rules for  $k_3$ .

$\delta\dot{\gamma} \backslash \dot{\gamma}$	NB	NM	NS	ZO	PS	PM	PB
NB	S	B	B	B	B	B	S
NM	S	B	B	B	B	B	S
NS	S	S	B	B	B	S	S
ZO	S	S	S	B	S	S	S
PS	S	S	B	B	B	S	S
PM	S	B	B	B	B	B	S
PB	S	B	B	B	B	B	S

**Table 4.** Fuzzy tuning rules for  $k_4$ .

$\delta\dot{\gamma} \backslash \dot{\gamma}$	NB	NM	NS	ZO	PS	PM	PB
NB	S	S	S	S	S	S	S
NM	B	B	S	S	S	B	B
NS	B	B	B	S	B	B	B
ZO	B	B	B	B	B	B	B
PS	B	B	B	S	B	B	B
PM	B	B	S	S	S	B	B
PB	S	S	S	S	S	S	S

$$\mu_{i,k_3} = \mu_{\gamma}(\gamma_i) \cdot \mu_{\dot{\gamma}}(\dot{\gamma}_i) \dots \dots \dots (10)$$

$$\mu_{i,k_4} = \mu_{i,k_3} \dots \dots \dots (11)$$

where  $\mu_{\beta}(\beta_i)$  is the membership functions value of the fuzzy set of  $\beta$  at a value of  $\beta_i$  in Fig.5,  $\mu_{\dot{\beta}}(\dot{\beta}_i)$  is the membership function value of the fuzzy set of  $\dot{\beta}$  at a value of  $\dot{\beta}_i$  from Fig.5,  $\mu_{\gamma}(\gamma_i)$  is the membership function value of the fuzzy set of  $\gamma$  at a value of  $\gamma_i$  from Fig.5, and  $\mu_{\dot{\gamma}}(\dot{\gamma}_i)$  is the membership function value of the fuzzy set of  $\dot{\gamma}$  at a value of  $\dot{\gamma}_i$  from Fig.5.

Based on  $\mu_{i,k_1}$ ,  $\mu_{i,k_2}$ ,  $\mu_{i,k_3}$  and  $\mu_{i,k_4}$ , the values of  $k_1(i)$ ,  $k_2(i)$ ,  $k_3(i)$ , and  $k_4(i)$  for each rule are determined from their corresponding membership functions given in Fig.6. Then,  $k_1$ ,  $k_2$ ,  $k_3$ , and  $k_4$  are obtained in Eqs.(12)-(15) by the following defuzzification equations:<sup>15)</sup>

$$k_1 = \frac{\sum_{i=1}^n \mu_{i,k_1} k_1(i)}{\sum_{i=1}^n \mu_{i,k_1}} \dots \dots \dots (12)$$

$$k_2 = \frac{\sum_{i=1}^n \mu_{i,k_2} k_2(i)}{\sum_{i=1}^n \mu_{i,k_2}} \dots \dots \dots (13)$$

$$k_3 = \frac{\sum_{i=1}^n \mu_{i,k_3} k_3(i)}{\sum_{i=1}^n \mu_{i,k_3}} \dots \dots \dots (14)$$

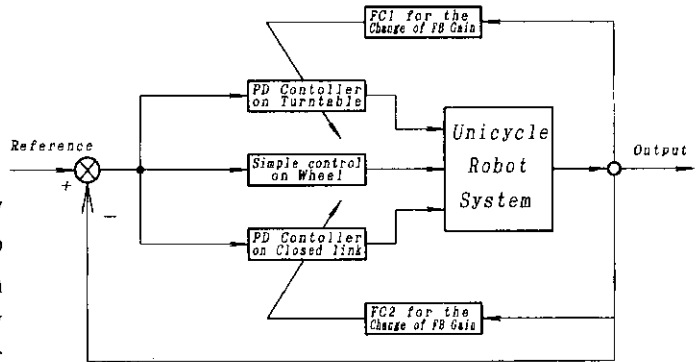


**Fig. 7.** Control block diagram.

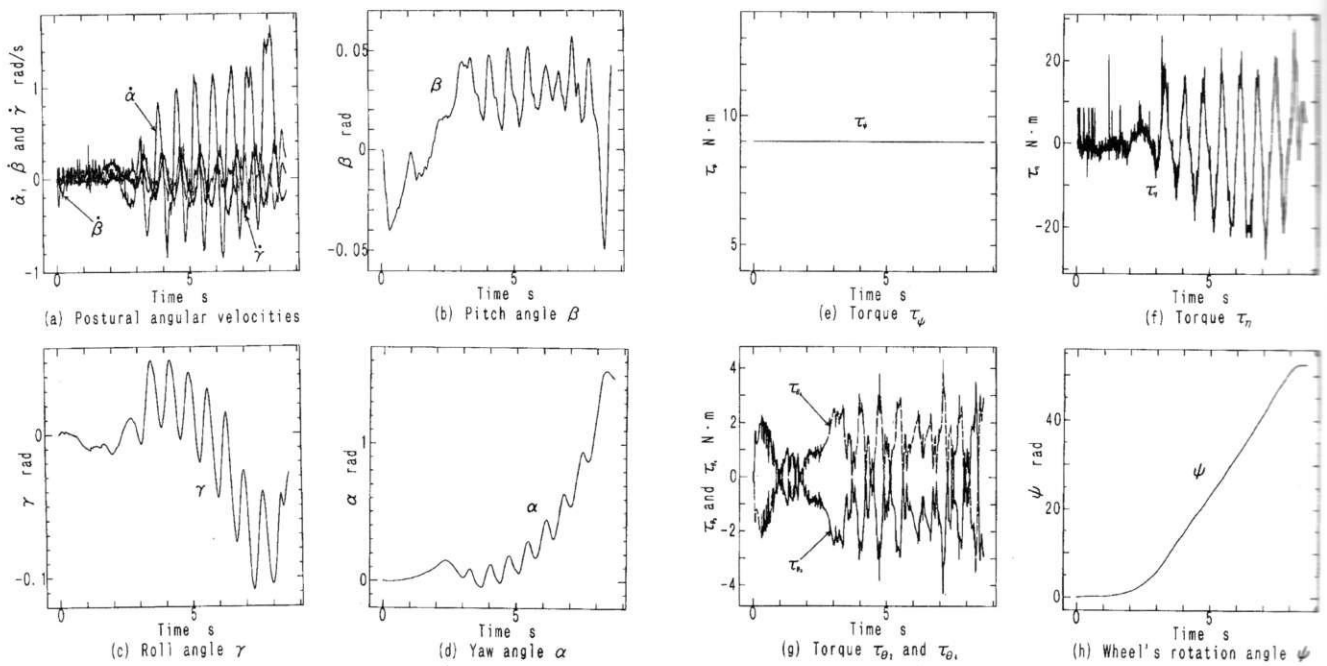
$$k_4 = \frac{\sum_{i=1}^n \mu_{i,k_4} k_4(i)}{\sum_{i=1}^n \mu_{i,k_4}} \dots \dots \dots (15)$$

With the proposed control method, we depict the control block diagram in Fig.7. The robot's postural stability both longitudinally and laterally was obtained on a 3.0m×9.0m synthetic rubber carpet. Experimental results indicate that the proposed method is quite active and valid for the unicycle robot's postural stability control.

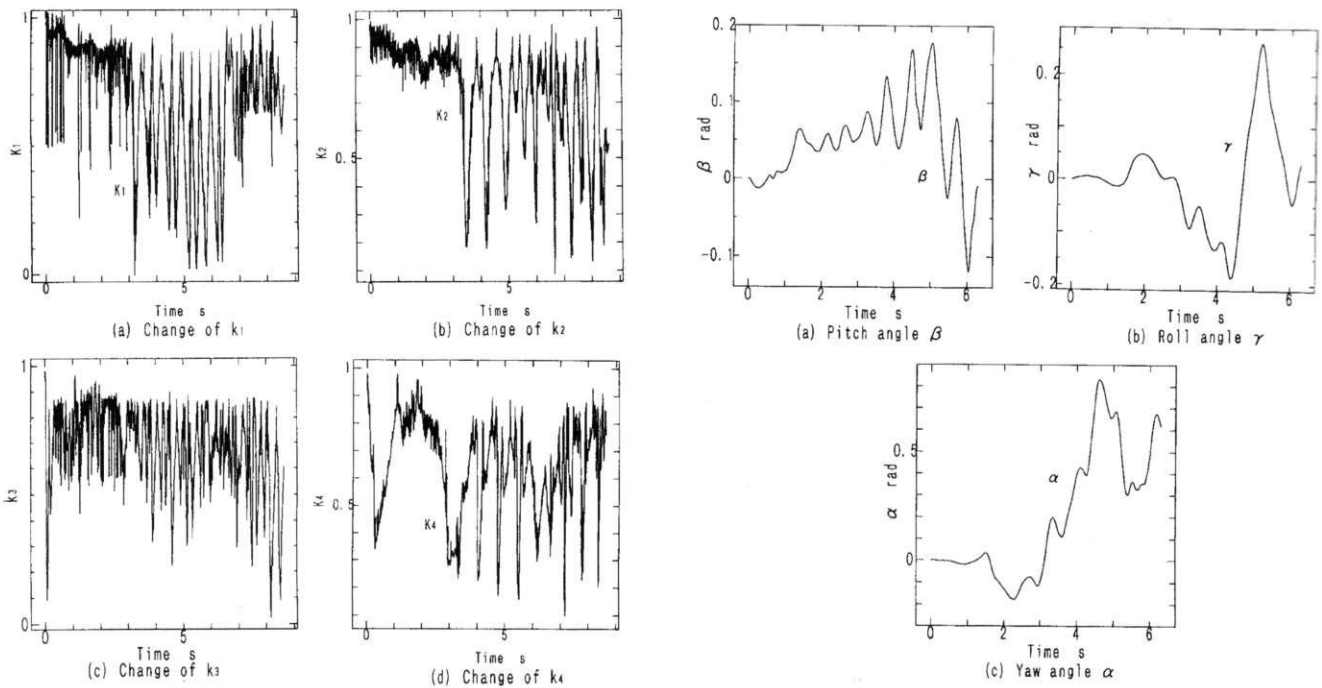
Since the unicycle robot's initial posture is set by the operator, and the ground's unevenness is random, we couldn't repeat just exactly the same result in the experiment even with the same control methods and same feedback gains. Two kinds of experimental result with the same control methods and same feedback gains are shown on Figs.8, 9, and 10. In these two experiments,  $kp_1 = 4000.0$ ,  $kd_1 = 400.0$ ,  $kp_2 = 800.0$ , and  $kd_2 = 2400.0$  are used, and the sampling time is taken as 5ms.

Figure 8(a) shows the changes of the robot's angular velocity with time in pitch, roll, and yaw direction.

The changes of robot posture in pitch, roll, and yaw direction are shown in Figs.8(b), (c), and (d). Figure 8(b) indicates that the robot's postural stability in the pitch direction (longitudinal stability) is obtained efficiently due to the active usage of the closed link mechanisms in this robot.



**Fig. 8.** Change of posture angles, postural angular velocities, torques and wheel's movement distance with time. (Experimental results obtained by two fuzzy gain schedule PD controller(I))



**Fig. 9.** Change of fuzzy parameters  $k_1, k_2, k_3$  and  $k_4$  with time. (Experimental results obtained by two fuzzy gain schedule PD controllers(I))

**Fig. 10.** Change of posture angles with time. (Experimental results obtained by two fuzzy gain schedule PD controllers(II))

Figure 8(c) shows the roll angle is changeable due to disturbance such as the ground's unevenness, and it can be stabilized near zero even though sometimes it reaches 0.11 rad. So, the robot's lateral stability (stability in the roll direction) is obtained. Figure 8(d) shows that the robot's posture in the yaw direction is changed quickly in the experiment. The reason is that yaw direction control is for achieving the robot's lateral stability, the change of the ground's unevenness will yield the robot's lateral posture change, and the change of the robot's lateral posture (change of robot roll direction) requires the robot's posture in the yaw direction to be changed.

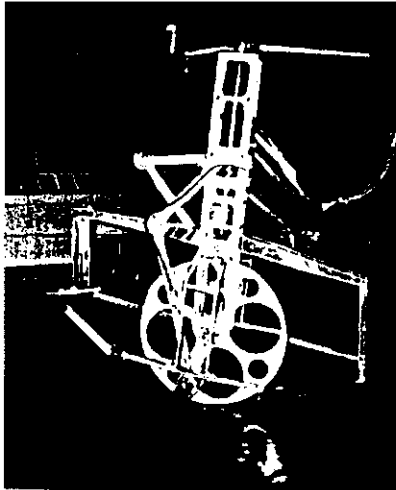


Fig. 11. Stable driving the robot.

The torques for wheel and rotor are shown in Fig.8(e) and 8(f). Figure 8(g) shows the torques for links 2 and 4.

Figure 8(h) displays the wheel's movement distance as well as its speed. The wheel's average speed is about 1.2m/s, similar to that of a rider riding a unicycle.

Figures 9(a)-(d) show the change of  $k_1$ ,  $k_2$ ,  $k_3$ , and  $k_4$  over time in experiment (I).

Figure 10 shows the change of posture angles  $\alpha$ ,  $\beta$ , and  $\gamma$  with time in experiment (II). From Fig.10(b), we know the robot's lateral stability can be obtained even though roll angle sometimes reach 0.28 rad due to the ground's unevenness. In fact, the robot's postural stability will be broken by PD and D controllers in the previous paper<sup>2)</sup> when the roll angle reaches 0.1 rad due to the ground's unevenness.

Figure 11 is a photo of the robot's posture in experiment.

In experiments, the initial posture of the robot is set by the operator, and the operator's hand is removed when the wheel begins to go forward. In the comparison with the experimental results reported in the previous paper,<sup>2)</sup> we know that it is much easier for achieving the robot's postural stability with the fuzzy gain schedule PD controller. If the set initial posture of the robot is not so far from the reference ideal stable posture ( $\beta = 0.0$  rad and  $\gamma = 0.0$  rad), postural stability can be obtained in almost all trials. Repeatability of the postural stability control by PD and one D controllers<sup>2)</sup> was poor when the posture was disturbed by the carpet's unevenness. However, the postural stability with two fuzzy gain schedule PD controllers can be achieved even if the posture is disturbed to some extent by the carpet's unevenness and so on. Therefore, experimental results show

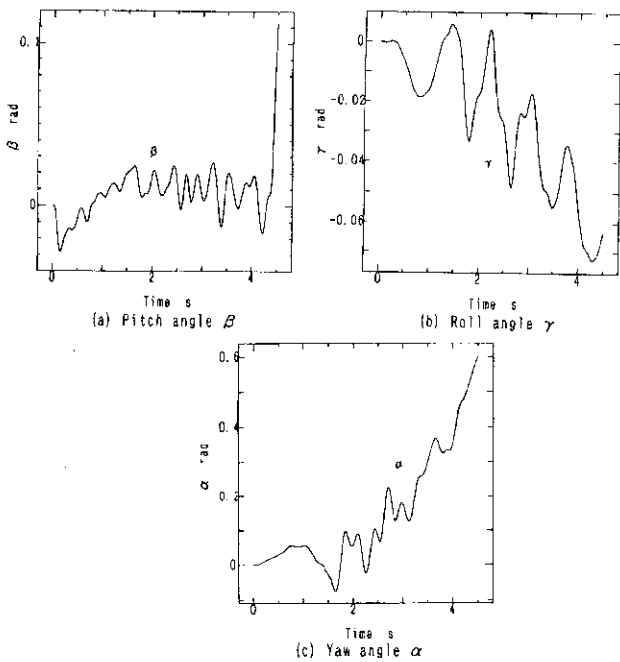


Fig. 12. Change of posture angles with time. Experimental results obtained by a PD + D controller)

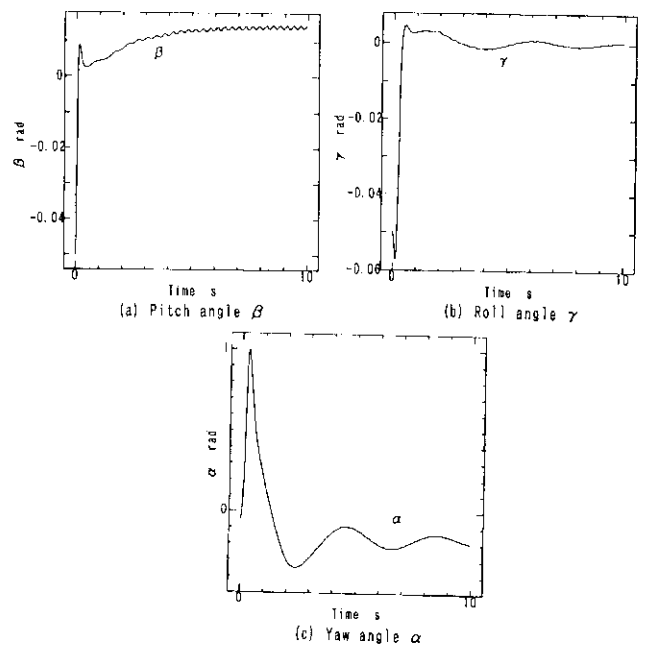


Fig. 13. Change of posture angles with time. (Simulation results obtained by two fuzzy gain schedule PD controllers)



**Table 5.** Comparison of resulting performance of different controllers.

<i>Method</i>	<i>Simulation</i>			<i>Experiment</i>			
	<i>Control-lability</i>	<i>Stable area</i>	<i>Stable period</i>	<i>Control-lability</i>	<i>Stable area</i>	<i>Stable period</i>	<i>Reaction to disturbance</i>
<i>Two PD controllers</i>	<i>Good</i>	<i>Small</i>	<i>Short</i>	<i>Good</i>	<i>Small</i>	<i>Short</i>	<i>Weak</i>
<i>One PD and one PD fuzzy gain schedule controllers</i>	<i>Better</i>	<i>Big</i>	<i>Longer</i>	—	—	—	—
<i>Two PD fuzzy gain schedule controllers</i>	<i>Much better</i>	<i>Big</i>	<i>Fair Long</i>	<i>Much better</i>	<i>Big</i>	<i>Longer</i>	<i>Strong</i>

that the proposed control is very effective in the improvement of the postural stability and controllability.

## 4. Discussions on Experimental Results

### 4.1. Comparison of Experimental Results with Those Obtained by PD + D Controller

The experimental results obtained with a PD + D controller<sup>2)</sup> are shown in Fig.12. Comparing Fig.12(a)-(c) with Figs.8(b)-(d), we see that better postural stability is achieved by a fuzzy gain schedule PD controller than by a PD + D controller. As seen in Fig.12(b), the roll angle is changed, on a small scale, but is not stabilized around zero, and tended to incline with time. Compared to Fig.12(b), the roll angle in Fig.8(c) is changed on a big scale, but it is stabilized around zero because the effective recovery torque is yield by the fuzzy gain schedule PD controller. In our experiment with the PD + D controller,<sup>2)</sup> the robot's postural stability often could not be kept if the roll angle was as big as the value in Fig.8(c), while the robot's postural stability can be recovered with the two fuzzy gained schedule PD controllers even though the roll angle become big. Such recovery shows the excellent characteristics of the two fuzzy gain schedule PD controllers.

### 4.2. Comparison with Simulation Results and Summarizing on the Simulation and Experimental Results

Part of simulation results with two fuzzy gain schedule PD controllers<sup>14)</sup> is shown in Fig.13. Comparing Figs.13(a)-(c) with Fig.8(b)-(d), we see these exists some similarity between the simulation and experiment on postural stability control. Figure 13(a) indicates that the pitch angle is stabilized around a value but not zero in the simulation. Figure 8(b) also shows the pitch angle is stabilized around a value but not zero in the experiment. Figure 13(b) indicates the roll angle is stabilized around zero in the simulation, Fig.8(c) also shows the roll angle is stabilized around zero in the experiment. Because of the unevenness of the synthetic rubber carpet, it is reasonable for us to have a result for the yaw angle as in Fig.8(d) in the experiment, although the yaw angle is not controlled to zero as shown in Fig.13(c).

Of course, as pointed out in the last section, because the robot's initial posture is set by the operator in the experiment, the influence caused by the hand in initial state is

inevitable. Furthermore, carpet unevenness will significantly influence the robot's postural stability. The mathematical model cannot describe such a contact condition and friction between the wheel and ground precisely. Therefore, it will be impossible for us to get exactly the same result as simulation by experiment. However, as shown above, we have gotten experimental results which are similar to simulation results, indicating the proposed method is effective in handling the system's nonlinearity for the robot's postural stability control.

We have done simulations and experiments on the improved unicycle model with different control in this paper together with the previous paper.<sup>2,3,13)</sup> Results are summarized in Table 5.

## 5. Conclusions

In this paper, the experiment on the stability and driving control of a unicycle robot is conducted on a synthetic rubber carpet with proposed fuzzy gain schedule PD control. Conclusions are summarized as follows:

- (1) The unicycle robot's postural stability and driving control are realized on a 3m×9m synthetic rubber carpet.
- (2) The experimental result shows that the proposed fuzzy gain schedule PD controller is valid for the robot's postural stability control.
- (3) The experimental result indicates that the proposed fuzzy gain schedule PD controller is better than the conventional PD controller for the robot's postural stability control.

### References:

- 1) Z. Sheng and K. Yamafuji, Study on the Stability and Motion Control of a Unicycle (1st Report: Dynamics of a human riding a unicycle and its modeling by link mechanism), JSME International Journal, Series C, **38-2**, 249-259 (1995).
- 2) Z. Sheng and K. Yamafuji, Study on the Stability and Motion Control of a Unicycle (2nd Report: Design of unicycle report and experimental results), Japan Society of Mechanical Engineering, **61-583C**, 1042-1049 (1995) (in Japanese).
- 3) Z.Q. Sheng, K. Yamafuji and S.V. Ulyanov, Study on the Stability and Motion Control of a Unicycle (3rd Report: Characteristics of Unicycle Robot, JSME International Journal, Series C, **39-3**, 560-568 (1996).
- 4) S. Hayashi, "A Tuning Method of Fuzzy Control System," Proc. of 6th Fuzzy System Symposium, Tokyo 189-192 (1990).

- 5) C. Lee, "Fuzzy Logic in Control Systems: Fuzzy Logic Controller – Part I," IEEE Transactions on Systems, Man, and Cybernetics, **20-2**, 404-418 (1990).
- 6) C. Lee, "Fuzzy Logic in Control Systems: Fuzzy Logic Controller, Part II," IEEE Transactions on Systems, Man, and Cybernetics, **20-2**, 419-435 (1990).
- 7) K. Tanaka and M. Sano, "Parameter Adjustment Laws of Fuzzy Controllers for First Order Lag System with Dead Time," J. of Japanese Society for Fuzzy Theory and Systems, **3-3**, 583-591 (1991).
- 8) A. Kandel, L. Li and Z. Cao, "Fuzzy Interface and Its Applicability to Control Systems," Fuzzy Sets and Systems **48**, 99-111, North-Holland (1992).
- 9) Bimal K. Bose, "Expert System, Fuzzy Logic, and Neural Network Applications in Power Electric and Motion Control," Processing of the IEEE, **82-8**, 1303-1323 (1994).
- 10) V.N. Zakharov and S.V. Ulyanov, "Fuzzy Models of Intelligent Industrial Controllers and Control Systems, II. Evolution and Principles of Design," Journal of Computer and Systems Sciences International, **33-2**, 94-108 (1995).
- 11) V.N. Zakharov and S.V. Ulyanov, "Fuzzy Models of Intelligent Industrial Controllers and Control Systems, III. Design Procedure," Journal of Computer and Systems Sciences International, **33-2**, 117-135 (1995).
- 12) Jerry M. Mendel: "Fuzzy Logic Systems for Engineering: A Tutorial", Proceeding of the IEEE, **83-3**, 345-377, 1995.
- 13) Z.Q. Sheng, K. Yamafuji and S.V. Ulyanov, Study on the Stability and Motion Control of a Unicycle (4th report: Fuzzy Gain Schedule PD Controller for Managing Nonlinearity of System), JSME International Journal, Series C, **39-3**, 569-576 (1996).
- 14) Z. Sheng and K. Yamafuji, Realization of a Human Riding a Unicycle by a Robot, '95 IEEE International Conference on Robotics and Automation, Nagoya 1319-1326 (1995).
- 15) M. Sugeno, Fuzzy Control, Japan Industry News Press (in Japanese) (1989).



**Name:**  
Zaiquan Sheng

**Affiliation:**  
Dr. of Engineering, Researcher in Endress+Hauser International Group Computing and University of Electro-Communications

**Address:**  
1-5-1 Chofugaoka, Chofu, Tokyo, 182 Japan

**Brief Biographical History**

1987 - B.S. from University of Electronic Science and Technology of China  
 1990 - M.S. from University of Electronic Science and Technology of China  
 1995 - Dr. of Engineering, from University of Electro-Communications  
 1995 - Researcher in Endress+Hauser International Group Company

**Main Works:**

- Robotics and Mechatronics
- Factory Automation
- Automatic Measurement instrument
- Analog and Digital hard ware
- MCPU Application Software
- PLC (SFC) Technology

**Membership in Learned societies:**

- Japan Society of Mechanical Engineering
- Robotics Society of Japan et al.

**Name:**  
Ulyanov Sergei V. (see pp.553)

**Name:**  
Kazuo Yamafuji (see pp.554)